Scientific paper

Relationship between Nonlinear Creep and Cracking of Concrete under Uniaxial Compression

Miguel Fernández Ruiz[1], Aurelio Muttoni[2] and Pietro G. Gambarova[3]

Received 14 March 2007, accepted 2 July 2007

Abstract

This paper investigates the nonlinear creep behaviour of concrete in compression and its relationship with cracking under uniaxial compression (cracks developing parallel to the loading direction). A physical model explaining the nature and the role of linear and nonlinear creep strains is presented, together with a failure criterion for concrete under sustained loads. The model assumes that all nonlinear creep strains are due to concrete micro-cracking. The soundness of this assumption is checked against the experimental results obtained by the authors and by other researchers. The proposed model is shown to fit quite well the experimental results, for various load patterns and concrete ages.

The model also proves that the affinity hypothesis between linear and nonlinear creep strains (usually taken for granted in the design for stress levels below 70% of concrete strength in compression) is no longer valid when concrete fails under a sustained load, because of the unstable growth of cracking. Concrete response in these cases is analyzed in detail and a simplified but realistic approach for the evaluation of the failure envelope in compression is proposed.

1. Introduction

The effects of high stress levels on concrete long-term behaviour in compression are important with reference not only to the delayed strains, but also to the strength of the material. This topic was first studied by Rüsch (1960), who identified two regimes in concrete subjected to a sustained load, the first characterized by a "failure limit" (when the specimen fails by concrete crushing after a certain period after the application of the load) and by a "creep limit" (below which linear and nonlinear creep strains develop, but concrete does not fail, see **Fig. 1**).

Research on the creep limit – including the development of nonlinear delayed strains – has continued with several contributions covering a number of experimental and modelling issues. For design purposes, the attention has mainly focused on how to correct the linear creep coefficient (valid for $\sigma_c/f_c < 40$ %), taking advantage of the "affinity hypothesis" (i.e. proportionality between the linear and nonlinear creep coefficients, see **Fig. 2**), as shown for instance by Avram *et al*. (1981), and Fernández Ruiz *et al*. (2004) with satisfactory results. Formulae quantifying the influence of nonlinear creep strains and based on this approach were also adopted by some codes of practice (see for instance CEB MC 90).

Concerning the failure in compression under a sustained load, its origin has been associated with the development and growth of micro-cracking (Neville, 1970), but it has been shown (Mazzotti and Savoia, 2003) that only a fraction of the total delayed strains developing inside the concrete is due to cracking or, in other words, are related to material damage. A suitable approach for investigating the post-peak region has been presented in El-Kashif and Maekawa (2004) based on a coupled plasticity-damage model. Such approach can also include cyclic-loading effects (Maekawa and El-Kashif, 2004)

Similar conclusions on concrete strength under sustained loading or under increasing loading (with various loading rates) have been drawn for concrete subjected to bending and to tension (Bažant and Gettu, 1992; Bažant and Li, 1997a,b). In these cases, satisfactory results have been obtained using models that assume linear viscoelasticity for the creep in the undamaged concrete, and a rate-dependent formulation for crack development (van Zijl *et al*., 2001; Barpi and Valente, 2002), even in the postpeak phase (Barpi and Valente, 2005).

Here, a model for studying both the creep and the failure limits in concrete under sustained compression is presented, the aim being to investigate the effects of micro-cracking on concrete delayed strains and failure.

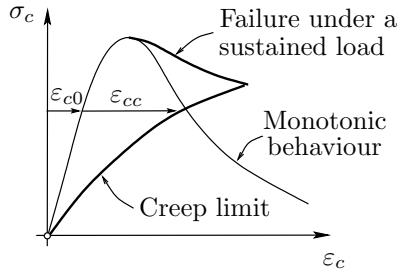

Fig.1 Sustained-load envelope for concrete in uniaxial compression: creep limit and failure limit according to Rüsch (1960).

[1]Post-doctoral fellow, Ecole Polytechnique Fédérale de Lausanne, Switzerland.
E-mail: miguel.fernandezruiz@epfl.ch
[2]Professor, Ecole Polytechnique Fédérale de Lausanne, Switzerland.
[3]Professor, Politecnico di Milano, Italy.

The model is checked against the results of an experimental campaign carried out on plain-concrete cylinders at the Structural Concrete Laboratory of EPFL (Ecole Polytechnique Fédérale de Lausanne, Switzerland). Specimens size Ø×*h* is 160×320 mm. Reference is made to two different concrete ages and to various loading patterns.

This research is significant with reference to both the ultimate and the serviceability limit states where reinforced and prestressed concrete structures are locally subjected to very large stresses. For instance, the concrete in contact with the ribs of bonded bars or with the end-plates of the tendons in prestressed concrete structures can locally be subjected to very large stresses that cause sizable stress redistributions in the surrounding (less stressed) concrete. These stress redistributions are favoured by the short–term development of inelastic strains. Understanding the behaviour of the concrete in these zones requires the detailed assessment of short-term creep strains and of their interaction with cracking, damage and plasticity. The proposed model not only fits quite well the test results obtained by the authors and by other researchers, but it also provides a clear explanation of the nature of the different components of the strain. It has the further advantage of being rather simple.

2. Theoretical model

Concrete exhibits a rheological behaviour consisting of delayed strains caused by different processes, whose origin is to be found in the microstructure of concrete. Conventionally, these strains are separated into shrinkage and creep strains, the former – shrinkage – comprising the strains that appear when no external loads are applied, and the latter – creep – comprising the delayed strains associated with the application of external loads (creep strains are defined as the difference between the total delayed strains and those caused by shrinkage). In spite of certain inconsistencies, this definition enables to quantify the phenomena in a simple way. For instance, in a concrete loaded at the age t_0 the strain at any given time t can be written as:

$$\varepsilon_c\left(t,\frac{\sigma_c}{f_c}\right)=\varepsilon_c\left(t_0,\frac{\sigma_c}{f_c}\right)+\Delta\varepsilon_{cs}(t,t_0)+\Delta\varepsilon_{cc}\left(t,t_0,\frac{\sigma_c}{f_c}\right) \quad (1)$$

where the creep strain can be obtained through a difference:

$$\Delta\varepsilon_{cc}\left(t,t_0,\frac{\sigma_c}{f_c}\right)=\varepsilon_c\left(t,\frac{\sigma_c}{f_c}\right)-\varepsilon_c\left(t_0,\frac{\sigma_c}{f_c}\right)-\Delta\varepsilon_{cs}(t,t_0) \quad (2)$$

As a rule, the creep strain is expressed in the following way:

$$\Delta\varepsilon_{cc}\left(t,t_0,\frac{\sigma_c}{f_c}\right)=\varepsilon_c\left(t_0,\frac{\sigma_c}{f_c}\right)\cdot\varphi\left(t,t_0,\frac{\sigma_c}{f_c}\right) \quad (3)$$

where $\varphi\left(t,t_0,\frac{\sigma_c}{f_c}\right)$ is the creep coefficient of concrete, which comprises the effect of both drying and basic creep.

By definition, shrinkage strains are independent of the stress state in the material. On the other hand, creep is directly related to concrete stresses and to micro-cracking. For any stress level below $0.4f_c$, creep strains can be described by means of a stress-independent formulation of the creep coefficient: $\varphi_{lin}(t,t_0)$. Consequently, creep strains are linearly related to the stresses. However, at higher stress levels this linearity is lost and the creep coefficient is no longer stress-independent (**Fig. 2**).

Various relationships have been proposed to describe the nonlinear effects of stresses on the creep coefficient. Based on the tests performed at stress levels below 70% of concrete compressive strength, a satisfactory fitting can be obtained by using the so-called affinity hypothesis. This hypothesis assumes that the linear and nonlinear creep strains are related through the actual stress ratio σ_c/f_c (see **Fig. 2**). This hypothesis can be written as follows:

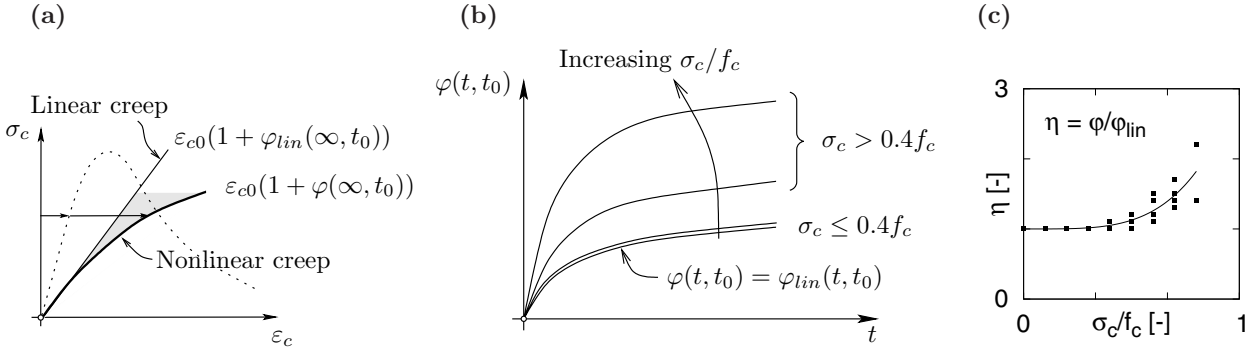

Fig. 2 (a) Linear and nonlinear creep strains; (b) creep coefficient for various values of the stress/strength ratio; and (c) plot of the affinity coefficient η (Eq. 5) for nonlinear creep, together with the test results by different authors (Fernández Ruiz, 2003).

$$\Delta\varepsilon_{cc} = \varepsilon_c(t_0)\cdot\varphi\left(t,t_0,\frac{\sigma_c}{f_c}\right) = \varepsilon_c(t_0)\cdot\varphi_{lin}(t,t_0)\cdot\eta\left(\frac{\sigma_c}{f_c}\right) \quad (4)$$

where the "affinity coefficient" η can be given a polynomial formulation, as recently proposed by the first author (2003) with reference to the ascending branch of the stress-strain curve:

$$\eta = 1 + 2\cdot\left(\frac{\sigma_c}{f_c}\right)^4 \quad (5)$$

As shown in **Fig. 2c**, Eq. (5) fits rather well the values worked out from several tests. This expression has satisfactorily been used for both creep and relaxation problems, using an extension of the aging-coefficient method (Fernández Ruiz, 2003).

Going back to the strains in the concrete, instantaneous plastic strains develop as a result of the loading process, as shown in **Fig. 3**, where the uniaxial stress-strain response of a concrete specimen monotonically loaded up to A exhibits the plastic strain $\varepsilon_{cp,0}$. Thereafter shrinkage strains develop, as well as creep strains if the load remains constant over time (strain $\Delta\varepsilon_c$, from A to B in **figure 3**). Should the specimen be further loaded, the point C, which is assumed to be on a "shifted" monotonic curve, would be reached. In B, the total strain consists in a number of contributions:

$$\varepsilon_{c,B} = \varepsilon_{cp,0} + \Delta\varepsilon_{cv} + \Delta\varepsilon_{cp} + \frac{\sigma_{c0}}{E_B} \quad (6)$$

where $\Delta\varepsilon_{cv}$ is the concrete viscous strain (time-related strain not associated with concrete micro-cracking = linear-creep strain + shrinkage strain) and $\Delta\varepsilon_{cp}$ the increase over time of the concrete plastic strains. The total strain increase ($\varepsilon_{c,B} - \varepsilon_{c,A}$) is:

$$\Delta\varepsilon_c = \Delta\varepsilon_{cv} + \Delta\varepsilon_{cp} + \left(\frac{1}{E_B} - \frac{1}{E_A}\right)\cdot\sigma_{c0} \quad (7)$$

In the following, concrete micro-cracking will be assumed to be the only source of the nonlinear part of the creep strain. Consequently, the total strain can be written as follows:

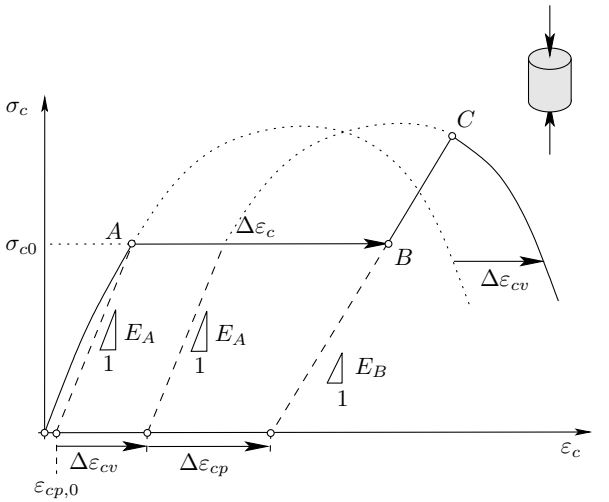

Fig. 3 Delayed strains caused by a sustained load.

$$\Delta\varepsilon_c = \underbrace{\Delta\varepsilon_{cv}}_{\varepsilon_c(t_0)\cdot\varphi_{lin}(t,t_0)+\Delta\varepsilon_{cs}(t,t_s)} + \underbrace{\Delta\varepsilon_{cp} + \left(\frac{1}{E_B} - \frac{1}{E_A}\right)\cdot\sigma_{c0}}_{\Delta\varepsilon_{cc,nl}} \quad (8)$$

where the nonlinear creep strain ($\Delta\varepsilon_{cc,nl}$) – representing the time-related inelastic strain – consists of the time-related plastic strain ($\Delta\varepsilon_{cp}$) plus a term ($(1/E_B - 1/E_A)\sigma_{c0}$) which represents the strain corresponding to the damage increase caused by micro-cracking ($E_B < E_A$).

This behaviour can be represented by means of the mechanical model shown in **Fig. 4a**, that represents a coupled plasticity-damage model with viscous strains where the damage is represented by the failure of the spring elements (a similar approach was followed by El-Kashif and Maekawa, 2004). **Fig. 4b** shows the response of the various elements of the model for the previously-studied load pattern (see **Fig. 3**).

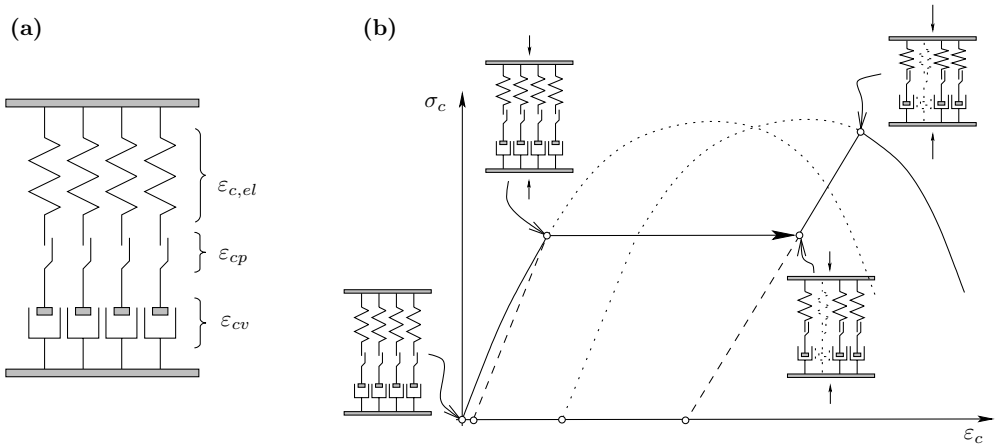

Fig. 4 Mechanical analogy: (a) mechanical model; and (b) response of the mechanical model at various loading states.

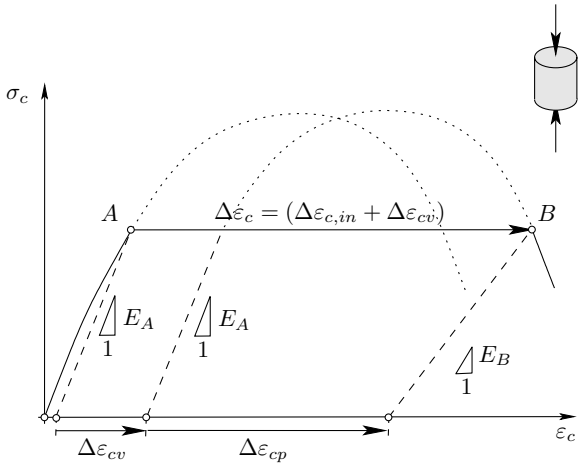

Fig. 5 Failure under a sustained load.

Concerning the development of the nonlinear creep strain, it has to be noted that if the inelastic strain capacity of the material ($\Delta\varepsilon_{c,in}$) is reached, the concrete fails by crushing under a constant load ($B \equiv C$), see **Fig. 5**.

3. Applicability of the affinity hypothesis

The development of the nonlinear creep strains can be evaluated in a simple way by means of Eq. (4), if the affinity hypothesis is introduced:

$$\Delta\varepsilon_{cc,nl} = \varepsilon_c(t_0) \cdot (\eta - 1) \cdot \varphi_{lin}(t, t_0) \tag{9}$$

As previously stated, this hypothesis provides good results for stress levels $\sigma_c/f_c < 0.70$. However, for larger stress levels (when concrete crushes under a sustained load), the actual development of nonlinear creep strains over time does not agree with the affinity hypothesis, see **Fig. 6**.

As later shown by the tests presented in this paper, three different phases can be identified for the nonlinear creep strains: (1) crack formation, (2) crack growth in a stable way, and (3) uncontrolled crack propagation up to concrete failure. In the first and second phases, the affinity hypothesis gives reasonable results (due to the convex shape of the curve –decreasing strain rate over time–), whereas in the third phase –unstable crack growth– sizable deviations from the affinity law are observed (due to the concave shape of the curve –increasing strain rate over time–).

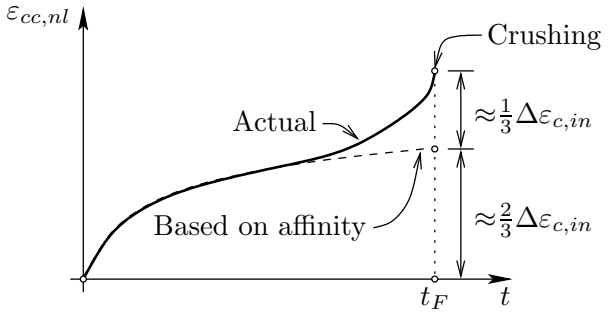

Fig. 6: Actual and affinity-based nonlinear creep strains.

In order to describe the development of the actual strain curve over time, that represents the concrete resistance to micro-cracking, the results of the tests under cyclic loading are helpful (since small-amplitude cycles are a way to force microcracking, which in turn produces a pseudo-plastic behaviour and damage in concrete). Although there are some phenomenological differences between both phenomena (Shah and Chandra, 1970) both phenomena can be treated in a unified manner as shown by Maekawa and El-Kashif (2004). **Fig. 7a** shows the typical cyclic response of concrete. The plastic strain evolution with the number of cycles (n) exhibits three phases as in the case of sustained loads. With reference to cyclic loading, the following analytical law is proposed to be adopted to characterize crack growth from crack formation to crack unstable propagation:

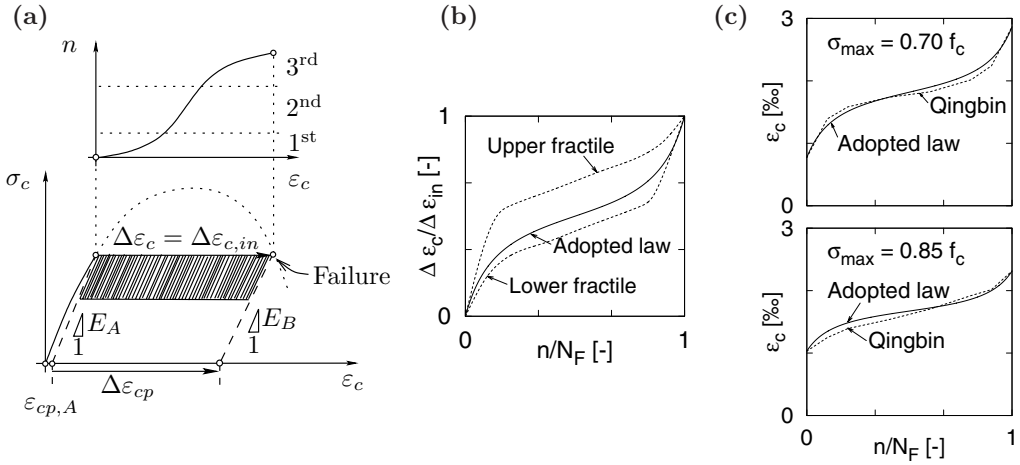

Fig. 7 Concrete response under cyclic loading: (a) typical behaviour; (b) plot of the proposed law and comparison with the fractile limits introduced by Pfanner *et al*. (2001); and (c) plots of the total strain as a function of the cycle numbers and comparison with the tests by Qingbin *et al*. (2004).

$$\Delta\varepsilon_{c,cyc} = \frac{\Delta\varepsilon_{c,in}}{2}\cdot\left[1+\zeta_n\cdot\frac{3-4\cdot\zeta_n^2}{(4\cdot\zeta_n^2-2)^2}\right] \quad \text{where}: \zeta_n = \frac{n}{N_F} - 0.5 \tag{10}$$

where $\Delta\varepsilon_{c,in}$ is the maximum allowable inelastic strain for a given load level. Many test data by various authors (Pfanner *et al*., 2001; Qingbin *et al*. 2004) have been successfully fitted with this equation (**Figs. 7b,c)**.

Equation (10) can also be used to characterize the development of nonlinear creep strains over time provided that the time to failure t_F (**Fig. 6**) is known. This parameter can be estimated by adopting the hypothesis that, at failure, 1/3 of the inelastic strain due to concrete micro-cracking provides from the unstable crack-growth phase (**Fig. 6**). Consequently, the maximum allowable inelastic strain can be obtained from the nonlinear creep strains based on the affinity hypothesis (Eq. (9)) as follows:

$$\Delta\varepsilon_{c,in} = \frac{3}{2}\cdot\left[\varepsilon(t_0)\cdot(\eta-1)\cdot\varphi_{lin}(t_F,t_0)\right] \tag{11}$$

where the value of t_F is the only unknown in Eq. (11) and can thus be evaluated. In spite of its simplicity, this formulation leads to a very good fitting of the test data.
As a result, for the cases where concrete fails in compression under a sustained load, the following expression for the development of nonlinear creep strains over time is proposed:

$$\Delta\varepsilon_{cc,nl} = \frac{\Delta\varepsilon_{c,in}}{2}\cdot\left[1+\zeta_t\cdot\frac{3-4\cdot\zeta_t^2}{(4\cdot\zeta_t^2-2)^2}\right] \quad \text{where}: \zeta_t = \frac{t}{t_F} - 0.5 \tag{12}$$

whereas in the cases when concrete does not fail under a sustained load, Eq. (9) based on the affinity hypothesis should be used to evaluate the nonlinear creep strains.

4. Experimental campaign

4.1. Objectives

This section presents the results of an experimental campaign performed by the authors at the Structural Concrete Laboratory of EPFL (Ecole Polytechnique Fédérale de Lausanne, Switzerland). The campaign has been carried out on plain-concrete, cylindrical specimens (size Ø×*h*=160×320 mm). Specimens were cast in two batches with the same mix design, see Table 1. A first set of specimens was tested 7-49 days after concreting, while a second set was tested eight months after concreting. Of course, the second set exhibited much smaller rheological effects. The properties of the specimens are summarized in **Table 2**.

The tests were performed using a Schenck Hydroplus 2500 kN, as well as two pairs of ordinary shrinkage and linear creep frames (**Fig. 8**). All tests were performed under controlled environmental conditions (relative humidity = 60 %, temperature = 22 °C).

Table 2 Specimens, concrete age and type of test/concrete grade. (*) Ordinary laboratory conditions: $\Delta\varepsilon_c/\Delta t \approx 10^{-5}$ sec^{-1}

Specimen	t_0 [days]	Type of test/Concrete grade
①	24	Failure under sustained load
②	27	Failure under sustained load
③	35	Failure under sustained load
④	36	Failure under sustained load
⑤	28/34	Nonlinear creep + reloading to failure
⑥	45	Nonlinear creep + reloading to failure
⑦	42	Nonlinear creep + reloading to failure
⑧	43	Nonlinear creep + reloading to failure
⑨	48	Relaxation steps
⑩	49	Relaxation steps
❶	7	Virgin curves* (f_c = 22.6 MPa)
❷	26	Virgin curves* (f_c = 30.2 MPa)
❸	34	Virgin curves* (f_c = 34.3 MPa)
❹	44	Virgin curves* (f_c = 33.7 MPa)
❺	47	Prefixed loading rate ($\dot{\delta} = 10^{-3}$ mm/sec)
❻	245	Prefixed loading rate ($\dot{\delta} = 10^{-2}$ mm/sec)
❼	245	Prefixed loading rate ($\dot{\delta} = 10^{-3}$ mm/sec)
❽	245	Relaxation steps
❾	245	Relaxation steps

Table 1 Composition of 1 cubic meter and results of tests on fresh concrete.

Sand (1-4 mm) [kg]	Gravel (4-8 mm) [kg]	Gravel (8-16 mm) [kg]	Cement [kg]	Water [kg]	Slump test [mm]	Flow table test [mm]
753	604	661	325	174	20	360

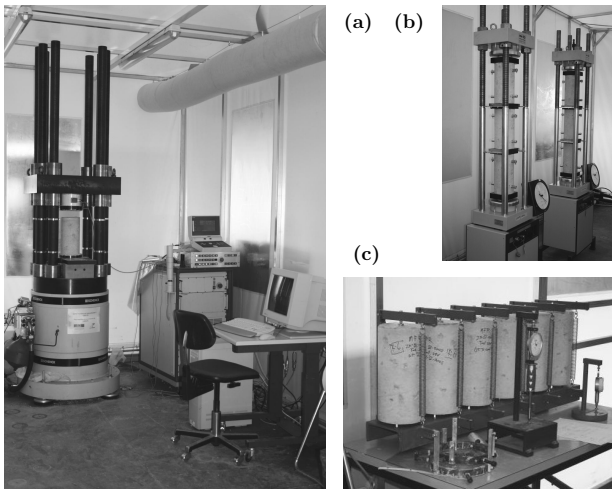

Fig. 8 Experimental set-ups: (a) Schenck Hydroplus with a capacity of 2500 kN; (b) linear-creep frames; and (c) shrinkage frames.

4.2. Nonlinear creep

Several specimens were subjected to a sustained load up to failure, with stresses ranging from $0.8 \cdot f_c$ to $0.9 \cdot f_c$, as shown in **Fig. 9**. Specimens ①, ② and ③ (sustained stress $\sigma_c = 0.9 \cdot f_c$) failed rapidly. Consequently, it may be assumed that almost all inelastic strains were due to concrete micro-cracking. These specimens exhibited a well-developed crack pattern at the end of the loading process all along the specimen. Furthermore, the width of the longitudinal cracks increased regularly during the test until failure. Regarding the strain rate (**Fig. 9b**), the above-mentioned three different phases can be easily identified: at first a rapid strain increase (and crack development), followed by a stable phase where the strain rate is approximately constant; finally on the unstable phase, in which both the strains in the solid concrete and the cracks become uncontrolled.

Specimen ④ exhibited the same failure pattern, but – since the stress level was lower and the load was applied for a much longer period – linear creep strains developed as well. These viscous strains (evaluated on the basis of the results obtained by the authors on concrete specimens exhibiting only linear-creep strains, $\sigma_c < 0.4 \cdot f_c$), are plotted in **Fig. 9c** (dashed line), where one can note that the curves are not proportional especially in the phase of unstable crack growth. Since the linear-creep strains do not contribute to the cracking of the specimen, the development of these strains seems to be the reason why, contrary to the other specimens, the failure of specimen ④ occured outside the monotonic curve (which in this case is represented by specimen ❹).

Fig. 10 shows the results obtained with specimen ⑤, which was loaded to failure after being loaded for six days at the stress level $\sigma_c/f_c \approx 0.60$. The specimen developed appreciable nonlinear creep strains at the beginning of the loading process, with an increase in the number and width of the cracks. However, its response became stable at a later stage, and no additional cracks

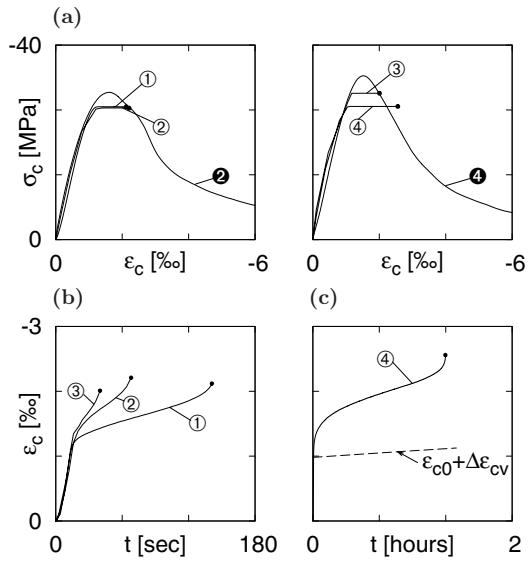

Fig. 9 Concrete failure under a sustained load: (a) stress-strain diagrams for specimens ① - ④ ; and (b,c) plots of the strains as a function of the time: (b) σ_c/f_c = 0.90, and (c) σ_c/f_c = 0.80.

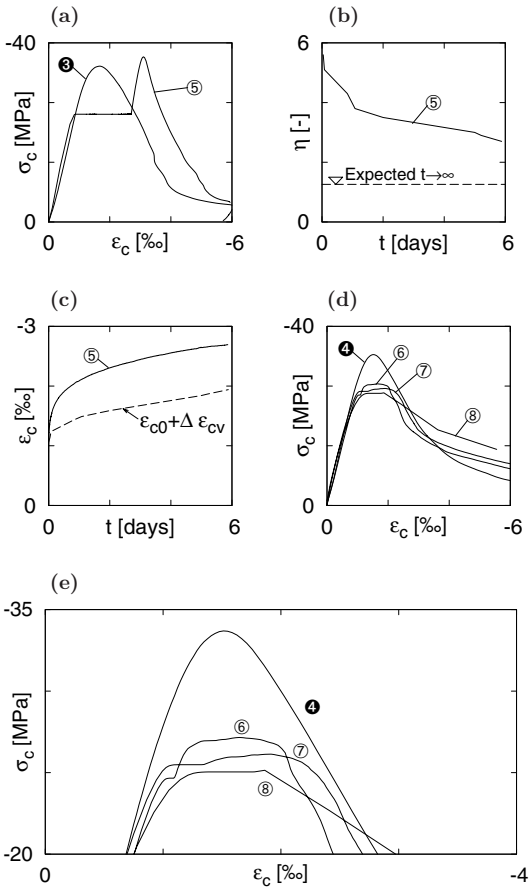

Fig. 10 (a) Stress-strain diagram of specimen ⑤; (b) affinity coefficient ($\eta = \varphi/\varphi_{lin}$, specimen ⑤); (c) development of the strains over time of specimen ⑤; (d) stress-strain curves of specimens ⑥ - ⑧ reloaded after a period of sustained loading; and (e) detail of the previous plot.

appeared (neither did their width significantly increase).

Comparing the total strains with the linear-creep strains (obtained from some linear-creep specimens loaded in the same day, see the dashed line in **Fig. 10c**) it can be seen that between 2 and 6 days (onset of reloading) the delayed strains of the specimen were almost those corresponding to linear creep. The time-related evolution of the affinity coefficient η can also be observed in **Fig. 10b**, where the values are very large at the beginning, and then quickly decrease and stabilise. The expected asymptote (for time) would be close to $\eta = 1.3$, if the remaining part of the nonlinear strain is neglected compared to the linear-creep strain, as suggested by the trend shown over the last days. Such value is calculated assuming that the linear creep coefficient at time infinite is $\varphi(\infty,28) = 2.2$ (obtained by adjusting the creep expression of the MC-90 to the test results) and by introducing $\varepsilon_c(t_0) = 1$ ‰ and $\Delta\varepsilon_{cc,nl} = 0.77$ ‰ (obtained from **Fig. 10c**) into eq. (9):

$$\eta = \frac{\varphi}{\varphi_{lin}} = \frac{\varepsilon_c(t_0)\cdot\varphi_{lin} + \Delta\varepsilon_{cc,nl}}{\varepsilon_c(t_0)\cdot\varphi_{lin}} = \frac{1.0\cdot 2.2 + 0.77}{1.0\cdot 2.2} = 1.3 \tag{13}$$

The value $\eta = 1.3$ is in good agreement with other theoretical predictions based on the affinity hypothesis ($\eta = 1 + 2\cdot(\sigma_c/f_c)^4 = 1.25$, see Eq. (5)).

Finally, several tests were carried out with the same loading history as specimen ⑤ (sustained load + reloading), but with higher initial stress levels, in order to shorten the time to failure under sustained loading. These specimens were left to develop nonlinear creep strains for less than five minutes. The results shown in Figs. 10d,e refer to three specimens, where the load was increased at different phases of the nonlinear creep process, so as to observe the typical behaviour of Phase 1 (crack development, specimen ⑥), Phase 2 (stable crack growth, specimen ⑦) and Phase 3 (unstable crack propagation, specimen ⑧). The results show that after the development of some nonlinear creep strains, the specimen remains capable of carrying additional loads. However, the previous load history is remembered and the stress increase depends on the amount of inelastic strains developed during the nonlinear creep phase. Furthermore, during the reloading process, the stiffness is similar to that in the elastic domain, with the concrete still undamaged or only slightly damaged. However, when concrete is considerably cracked, nonlinear-creep strains develop during the reloading process and the apparent stiffness is smaller.

4.3. Influence of the loading rate

An analogy may be established between the effects of a sustained load and of the loading rate on the failure of the material. Loading-rate effects were studied by Rüsch (1960) and are currently considered by some codes (for instance CEB MC 90).

Some tests have been carried by the authors, by changing the rate of the imposed displacement (δ) on several specimens. These tests were performed on the same concrete, but at different ages (1.5 months and 8 months, set 1 and set 2 in the following) and at different displacement rates ($\dot{\delta} \propto 10^{-3}$ mm/sec and $\dot{\delta} \propto 10^{-2}$ mm/sec). The results are shown in **Fig. 11**.

Both sets exhibited a similar behaviour characterized by a smaller peak stress (= strength) when the loading

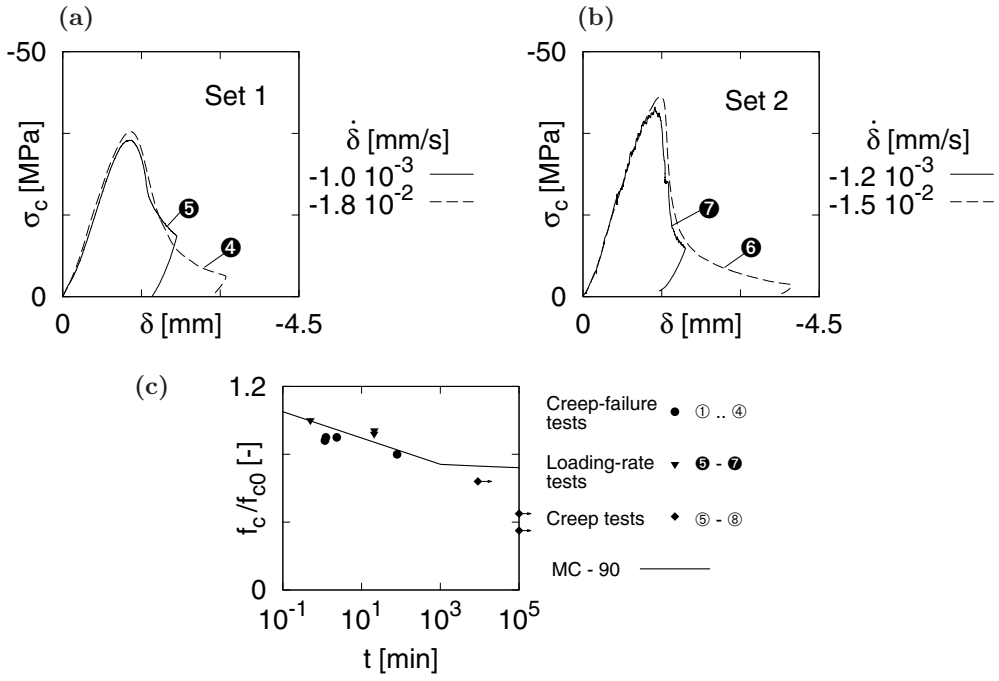

Fig. 11 Test results of the influence of the loading-rate on concrete strength: (a) set 1; (b) set 2; and (c) plot of concrete non-dimensional compressive strength as a function of the loading time.

rate was lower. This seems reasonable, since lower rates imply that the load is applied over a greater period of time, thus giving the cracks the possibility to open and to propagate in the same way as in pure-creep tests, up to the failure of the material (this is also an explanation of the similar behaviours of the young concrete –set 1– and of the older concrete –set 2–). However, the development of micro-cracking (which was considered in the proposed model to depend on the ratio σ_c/f_c) is not as fast under an increasing load as in a pure creep test in which the load is sustained (i.e. applied at its maximum value since the beginning of the test). This is logical since cracks propagate from the beginning of the test in pure creep tests but not in loading rate tests.

The results obtained with different loading rates are compared in **Fig. 11c**, along with those concerning nonlinear creep tests and the MC-90 loading rate formulation. One should note that in the nonlinear creep tests a lower strength is obtained than in the corresponding loading-rate tests. This confirms previous considerations on the development of micro-cracking.

4.4. Role of cracking

To study the development of cracking in a nonlinear rheological process, four specimens were subjected to multiple relaxation steps (i.e. unloading at constant displacement between the plates of the hydraulic jack). At each step, the number of cracks and their width were recorded by measuring the crack widths at the surface of the specimen using a manual crack comparator. The results (**Fig. 12**) show that cracking has a sizeable influence at stress levels above 60 % of the compressive strength. The relaxation due to nonlinear creep is remarkable and pseudo-plastic strains develop as cracking progresses, as confirmed by the investigation on the concrete tested at different ages (48 days and eight months). As already observed, the influence of concrete age is minimal, because nonlinear creep strains developed during the relaxation process have mainly to do with concrete cracking.

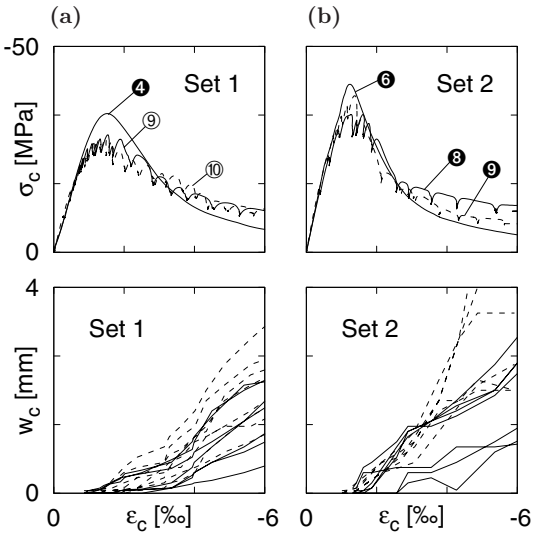

Fig. 12 Multiple relaxation steps: stress-strain diagrams and plots of the maximum crack width as a function of the mean strain, for: (a) set 1; and (b) set 2.

5. Fitting of test results

In **Fig. 13**, the proposed model is shown to fit rather well the results of the tests ① – ④. The monotonic envelope (comprising both the pre- and post-peak branches) is obtained using the expressions detailed in Appendix 1 of this paper. The points on the creep limit (comprising linear and nonlinear creep strains) are obtained assuming a linear creep coefficient equal to 2.2 (see section 4.2) for all specimens and using eq. (5) for estimating nonlinear creep strains.

The points representing failure under sustained load (comprising also linear and nonlinear creep strains) are obtained considering the available inelastic strain of the monotonic envelope and, as previously stated, assuming that failure develops when the nonlinear creep strain equals two thirds of the available inelastic strain. Thus, since the value of coefficient η is known from eq. (5), in light of eq. (11) the linear creep strains developed at failure can be estimated and consequently the total (linear + nonlinear) creep strains.

As shown in **Fig. 13**, the points representing concrete failure are very close to the envelope consisting of two curves, the upper with a softening branch (failure under sustained load) and the lower with a single increasing branch (creep limit). The development of the strain over time –as obtained with Eq. (12)– is further compared in

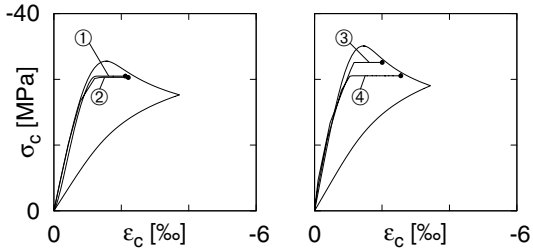

Fig. 13 Stress-strain curves for specimens ① – ④: compliance with the proposed sustained-load envelope.

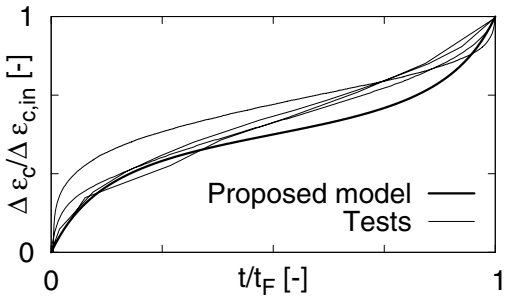

Fig. 14 Development of the delayed strains in specimens ① to ④, and comparison with the proposed theoretical model.

Fig. 14 with similar results.

For the part of the envelope related to the creep limit, the results shown in **Fig. 15**, with the reloading of specimen ⑤, exhibit a very satisfactory agreement between the viscous delayed strains and the strain increment obtained by shifting the monotonic curve to the right. This result perfectly agrees with the proposed theoretical model (**Fig. 3**).

Furthermore, for the reloading behaviour, the model is also in accordance with the results presented in **Figs. 10a,d,e** and **12**. The reloading modulus is similar to the elastic modulus whenever the inelastic strains (and subsequently the micro-cracking and damage of the material) are rather small, but it decreases at large inelastic strains.

The proposed model was also used to describe experimental results by Rüsch (1960). To this end, the affinity coefficient was evaluated by means of Eq. (5) and the analytical law describing the monotonic curve is detailed in Appendix 1. The fitting of the test results (**Fig. 16**) is very good indeed.

6. Parametric study

The influence of concrete short-term strength (f_c) and linear-creep coefficient on concrete long-term strength (f_c*, see **Fig. 17a**) is investigated in this section, taking advantage of the proposed model.

Concrete short-term strength is introduced with values ranging from 20 to 100 MPa. The corresponding stress-strain diagrams (**Fig. 17b**) are obtained by using the analytical laws detailed in Appendix 1 (assuming the same loading rate as in ordinary laboratory conditions: $\Delta\varepsilon_c/\Delta t \approx 10^{-5}$ sec^{-1}). Although developed for normal-strength concrete, the proposed model is applied here to high-strength concrete to study the effect of brittleness on concrete long-term strength (in other words, the behaviour of high-strength concrete is assumed to be similar to that of normal-strength concrete concerning nonlinear creep and micro-cracking).

Two cases are studied, with the same equivalent thickness ($e = 2A_c/u = 80$ mm, where A_c is the concrete cross-sectional area and u its perimeter) and loading time ($t_0 = 28$ days). The relative humidities are assumed to be 95% and 60% respectively; as a result, the linear creep coefficients are equal to 1.3 and 2.9 respectively for a concrete compressive strength of 30 MPa.

The results are compared with those by Rüsch (1960) and Fouré (1985) in **Fig. 17c**, where one should note that the ratio f_c*/ f_c is rather stable. Furthermore, the soundness of the value f_c*/ f_c = 0.85, taken for granted in practice and adopted from the experimental results of Rüsch (1960), is confirmed for f_c up to 30-40 MPa. It should be noted that this limit corresponds to average value and that a statistical analysis should be performed for determining the characteristic value of this limit.

Although the model has not been developed for

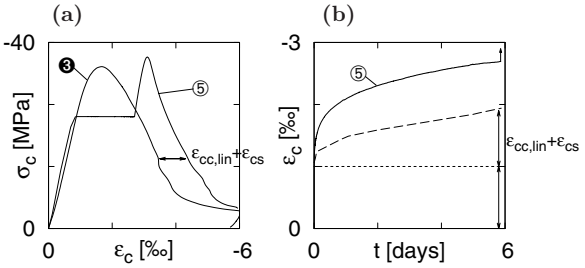

Fig. 15 Specimen ⑤: (a) stress-strain diagram; and (b) strain development over time.

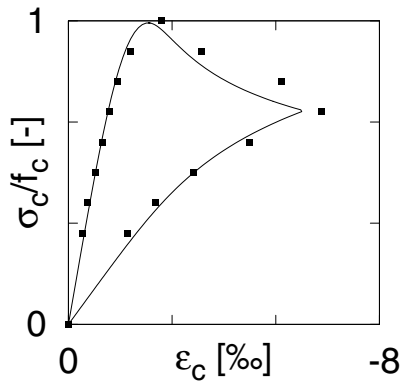

Fig. 16 Comparison of the proposed theoretical model with the test results by Rüsch (1960).

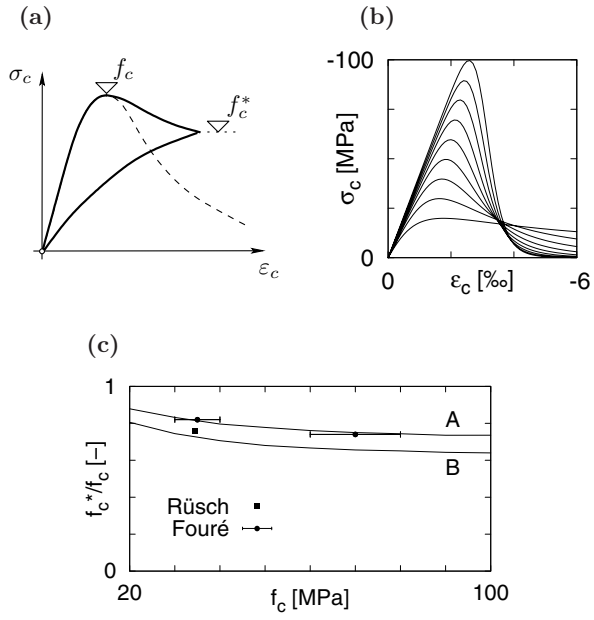

Fig. 17 Long-term strength of concrete: (a) definition of short- and long-term strengths, f_c and f_c* respectively (the dotted line is the monotonic post-peak envelope); (b) plots of the analytical stress-strain diagrams used in the parametric study; and (c) plots of f_c*/ f_c according to the proposed model and comparison with the experimental results of Rüsch (1960) and Fouré (1985); equivalent thickness 80 mm, loading time 28 days, relative humidity 95% (curve A) and 60% (curve B).

high-strengh concrete, a good agreement was also obtained with the test by Fouré for strengths up to 80 MPa. The f_c^*/f_c ratio clearly decreases in such cases, and limiting its value to 0.65 or 0.70 seems very reasonable. A reason for the decrease of the f_c^*/f_c ratio with f_c is found in the more brittle post-peak behaviour of high-strength concrete, which reduces the value of the inelastic strains ($\Delta\varepsilon_{c,in}$) that can be developed for a given stress/strength ratio. To limit this effect, the inelastic strain capacity of concrete should be increased (for instance by adding fibres or by introducing a confining pressure, see **Fig. 18**). In this way, the ratio f_c^*/f_c is increased as well.

In any case, more investigation on high strength concrete behaviour at high stress levels is required to check the applicability of the assumed hypotheses to other mixes since the crack initiation and nonlinear creep strain development may be different to those assumed in this paper for other matrices.

7. Conclusions

The relationship between nonlinear-creep strains and cracking in concrete is investigated in this paper to describe the possible failure of the concrete under sustained loading.

A physical model is proposed to describe the nonlinear creep strains that are assumed to have an inelastic nature and to be related to micro-cracking. A failure criterion is also proposed. According to this criterion, concrete crushes under a sustained load when no additional inelastic strains can be developed within the material for a given level of the stress.

An experimental campaign was carried out to validate the previous assumption on the nature of nonlinear-creep strains, and to check the reliability and accuracy of the proposed model. The relationship between nonlinear creep and micro-cracking was confirmed by the measurements performed on the specimens subjected to a sustained load and to multiple-relaxation steps.

Furthermore, the proposed failure criterion leads to a quite satisfactory theoretical-experimental agreement for various concrete ages, loading paths and loading-reloading processes.

The soundness of the affinity hypothesis between the linear and nonlinear creep strains (commonly adopted in structural design) is also the subject of this study, that confirms the validity of the affinity hypothesis in the crack-development phase and in the stabilized-crack phase, where the shape of the strain-time curve is convex. However, this hypothesis cannot be introduced in the phase of unstable crack-growth, where the strain-time curve has a concave shape. In this case, an analytical law based on the resistance of the material to crack propagation is proposed in order to describe the development of the inelastic strains over time.

Finally, a parametric study based on the proposed model has shown that the long-term strength of concrete (currently assumed as 85% of the short-term strength) is likely to be unsafe for high-strength concrete. In such a case, the long-term strength of concrete should be decreased to 65-70% of the corresponding short-term strength, unless the inelastic strain capacity of the material is increased by adding fibres or by introducing a confining pressure.

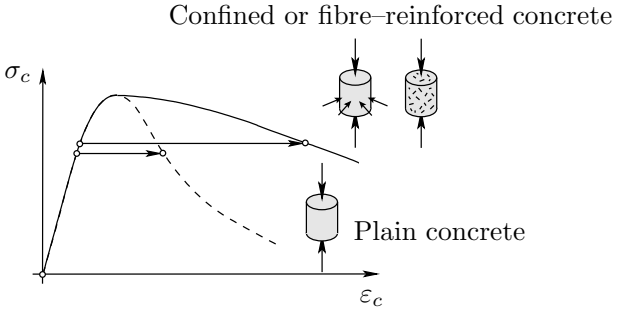

Fig. 18 Increase of the inelastic strain capacity of concrete by adding fibres or by introducing a confining pressure.

Appendix 1

The analytical stress-strain diagrams used in this paper have been obtained by using the following equation proposed by the authors:

$$\sigma_c = \frac{E_c \cdot \varepsilon_c}{1 + \left(\frac{\varepsilon_c}{\varepsilon_0}\right)^{\alpha}} \tag{14}$$

with ε_0:

$$\varepsilon_0 = \frac{\alpha \cdot f_c}{E_c \cdot (\alpha - 1)\left(1 - \frac{1}{\alpha}\right)} \tag{15}$$

and α:

$$\alpha = 0.5 + \frac{f_c\,[\mathrm{MPa}]}{20} + \frac{(f_c\,[\mathrm{MPa}])^2}{1500} \tag{16}$$

Notation

The following symbols are used in this paper:

E_c = modulus of elasticity of concrete
$E_{A,B}$ = modulus of elasticity of concrete (at A,B)
N_F = number of cycles at failure
f_c = concrete cylindrical strength in compression
n = number of cycles
t = time
t_0 = time at loading
$\Delta\varepsilon_{c,in}$ = maximum allowable inelastic strain for any given load level
δ = imposed displacement
$\dot{\delta}$ = displacement rate
ε_c = concrete strain
$\varepsilon_{c,el}$ = concrete elastic strain
ε_{cs} = concrete shrinkage strain

ε_{cp} = concrete plastic strain
ε_{cc} = total creep strain in concrete (= linear + nonlinear creep strains)
$\varepsilon_{cc,lin}$ = concrete linear-creep strain
$\varepsilon_{cc,nl}$ = concrete nonlinear creep strain (time-dependent strain associated with concrete micro-cracking = plastic strain + damage strain)
ε_{cv} = concrete viscous strains (time-dependent strain not associated with concrete mi cro-cracking = linear creep strains + shrinkage strains)
η = affinity coefficient
φ = creep coefficient
φ_{lin} = linear-creep coefficient
σ_c = concrete stress

References

Avram, C., Facaoaru, I., Filimon, I., Mirsu, O. and Tertea, I. (1981). "*Concrete strength and strain.*" Elsevier Scientific Publishing Company, Amsterdam –Oxford – New York, 558 p.

Barpi, F. and Valente, S. (2002). "Creep and fracture in concrete: a fractional order rate approach." *Engineering Fracture Mechanics*, 70, 611–623.

Barpi, F. and Valente, S. (2005). "Lifetime evaluation of concrete structures under sustained post–peak loading." *Engineering Fracture Mechanics*, 72, 2427-2443.

Bažant, Z. P. and Gettu, R. (1992). "Rate effects and load relaxation in static fracture of concrete." *ACI Materials Journal*, 89 (5), 456–468.

Bažant, Z. P. and Li, Y–N. (1997a). "Cohesive crack with rate–dependent opening and viscoelasticity: I. mathematical model and scaling." *International Journal of Fracture*, 86, 247–265.

Bažant, Z. P. and Li, Y–N. (1997b). "Cohesive crack with rate–dependent opening and viscoelasticity: II. Numerical algorithm, behavior and size effect." *International Journal of Fracture*, 86, 267–288.

CEB–FIP (1993). "Model code for concrete structures." Comité Euro–International du Béton, Lausanne, Switzerland, Thomas Telford Ltd., London, 460 p.

El-Kashif, K. F. and Maekawa, K. (2004). "Time-dependent nonlinearity of compression softening in concrete." *Journal of Advanced Concrete Technology*, 2 (2), 233-247.

Fernández Ruiz, M. (2003). "*Nonlinear analysis of the structural effects of the delayed strains of steel and concrete*." (in Spanish, "Evaluación no lineal de los efectos estructurales producidos por las deformaciones diferidas del hormigón y el acero"), PhD. Thesis, Universidad Politécnica de Madrid, Ed. ACHE, Madrid, Spain, 175 p.

Fernández Ruiz, M., Del Pozo Vindel, F. J. and Arrieta Torrealba, J. M. (2004). "*Nonlinear creep of concrete. analytical modelling and agreement with test results and previous theoretical models*." (in Spanish, Estudio sobre el comportamiento no lineal de la fluencia. Propuesta de modelo y comparación con resultados experimentales y modelos teóricos), Hormigón y Acero, 231, Madrid, Spain, 75–86.

Fouré B. (1985). "*Long–term strength of concrete under sustained loading*." (in French, Résistance potentielle à long terme du béton soumis à une contrainte soutenue), Annales de l'Institut Technique du Bâtiment et des Travaux Publics, 431, Paris, France, 45–64.

Maekawa, K. and El-Kashif, K. F. (2004). "Cyclic cumulative damaging of reinforced concrete in post-peak regions." Journal of Advanced Concrete Technology, 2 (2), 257-271.

Mazzotti, C. and Savoia, M. (2003). "Nonlinear creep damage model for concrete under uniaxial compression." ASCE, Journal of Engineering Mechanics, 129 (9), 1065–1075.

Neville, A. M. (1970). "Creep of concrete: Plain, reinforced and prestressed." Noth–Holland, Amsterdam, 622 p.

Pfanner, D., Stangenberg, F. and Petryna, Y. S. (2001). "*Probabilistic fatigue damage model for reinforced concrete*." Institute for reinforced and prestressed concrete structures, Ruhr–Universität Bochum, Bochum, 8 p.

Qingbin, L., Peiyin, L. and Lixiang, Z. (2004). "Damage degradation of concrete due to compressive fatigue loading." *Key Engineering materials*, 274–276, 123–128.

Rüsch, H. (1960). "Research toward a general flexural theory for structural concrete." *ACI Journal*, 57 (1), 1–28.

Shah, S. P. and Chandra, S. (1970). "Fracture of concrete subjected to cyclic and sustained loading." *ACI Journal*, 67 (10), 816-825.

van Zijl, G. P. A. G., Borst, R. and Rots, J. G. (2001). "The role of crack rate dependence in the long–term behaviour of cementitious materials." *International Journal of Solids and Structures*, 38, 5063–5079.